


5-2023

## The Impact of Glacial Proximity on the Elemental Composition of Leachate Derived from Sediment Weathering

Karoline Ford

Follow this and additional works at: [https://digitalcommons.unomaha.edu/university\\_honors\\_program](https://digitalcommons.unomaha.edu/university_honors_program)

 Part of the [Biogeochemistry Commons](#), [Environmental Chemistry Commons](#), [Geochemistry Commons](#), [Geology Commons](#), [Glaciology Commons](#), [Other Chemistry Commons](#), and the [Other Environmental Sciences Commons](#)

Please take our feedback survey at: [https://unomaha.az1.qualtrics.com/jfe/form/SV\\_8cchtFmpDyGfBLE](https://unomaha.az1.qualtrics.com/jfe/form/SV_8cchtFmpDyGfBLE)

The Impact of Glacial Proximity on the Elemental Composition of Leachate Derived from  
Sediment Weathering

Karoline Ford

University Honors Program — Senior Research Thesis

Dr. Kelly Deuerling

May 19, 2023

### Abstract

This study assesses chemical weathering trends as they relate to glacial retreat. The chemical environment of surfaces exposed to the atmosphere differs significantly from beneath a glacier. As a glacier melts, changes to the biogeochemical processes generate environmental gradients. This study analyzed chemical weathering signals at different distances from a glacial front by comparing the elemental composition of leachate derived from sediments in southeastern Greenland. Samples from proglacial, nonglacial, and moraine locations were weathered in a laboratory setting, and ion chromatography was used to determine the elemental composition of the products. Divergent trends in leachate composition were observed as distance from the glacial front changed. Evidence of gypsum and dolomite weathering was found in moraine sites. Proglacial sites contained higher ionic concentrations overall and did not yield the same weathering signals as moraine sites. Salt compositions also differed as a function of coastal proximity. This research offers a contribution to the scientific body of knowledge regarding the alteration of Earth cycles in response to a changing climate.

## Introduction

The term chronosequence refers to a series of environments occurring on similar substrate types with consistent climatic conditions, but that differ in the time since a disturbance— a retreating glacier generates a chronosequence. Glacial retreat provides a controlled setting to study biogeochemical cycling in soil and the emergence of ecological and geological progression. Glacial ice has existed for millions of years, keeping conditions relatively 'frozen' compared to the more rapid changes occurring in soil environments that are exposed directly to the atmosphere (Yu et al., 2023). Newly exposed ground has different accessible nutrients and environmental conditions compared to more weathered soil.

Weathering drives the generation of available ions in the sediment. In the glacial environment, coastal regions have been deglaciated for longer periods of time. The mineral reactivity of an exposed surface declines with age. This is because these regions have been exposed to weathering processes longer than recently deglaciated locations, and the supply of easily weathered minerals has been depleted. (Anderson, 2005). The carbonate minerals in these coastal regions are predominantly affected by sulfuric acid weathering. Carbonate minerals that are further inland towards the ice sheet are acted on more significantly by carbonic acid weathering (Deuerling et al., 2019). These broad trends in chemical weathering give rise to differences in nutrient and solute availability across the glacial foreland.

Elements mobilized by chemical weathering provide the nutrient foundation for developing ecosystems of microorganisms, as well as the available elements for the precipitation of new rock types. Microorganisms are critical to soil and carbon pool creation through nitrogen fixation and rock weathering processes, which also impacts regional geology

(Varliero, Anesio & Barker, 2021). In Greenland, nutrient and solute fluxes to the ocean are enhanced by glacial weathering (Hawkings et al., 2015) as well as elevated fluxes of potentially bioavailable forms of the micronutrient iron (Bhatia, 2013 & Hawkings, 2014).

This study assessed sediments at different points along the glacial chronosequence and with different watershed relationships to the glacier (nonglacial, proglacial, and moraine). These sediments were artificially weathered in the laboratory, and ion chromatography was used to determine the elemental composition of the resulting leachates.

## Methods

### *Field Site Description*

The field site analyzed in this study is located in southeastern Greenland (65° N, 37° W). The mean annual temperature is -1.7° C, with the mean January temperature at -7.5° C and the mean July temperature at 6.4° C. The region has sunshine for 1374 hours annually. Precipitation events occur on 32% of days each year, with a mean annual precipitation of 984 mm (Ernstsen, 2023). The region is a low arctic coastal vegetation zone, in an alpine shrubland habitat. The sampled sites consist of proglacial, nonglacial, and moraine sediments, located to the west of the retreating glacial ice cap that was originally connected to the Greenland Ice Sheet. Mittivakkat Gletscher, the outlet glacier in the region, has been in retreat for around 200 years. The general rock types are biotite and garnet-rich gneisses from the Ammassalik Intrusive Complex (Pedersen et al., 2013). The distance of each site from the glacier is shown in Table 1.

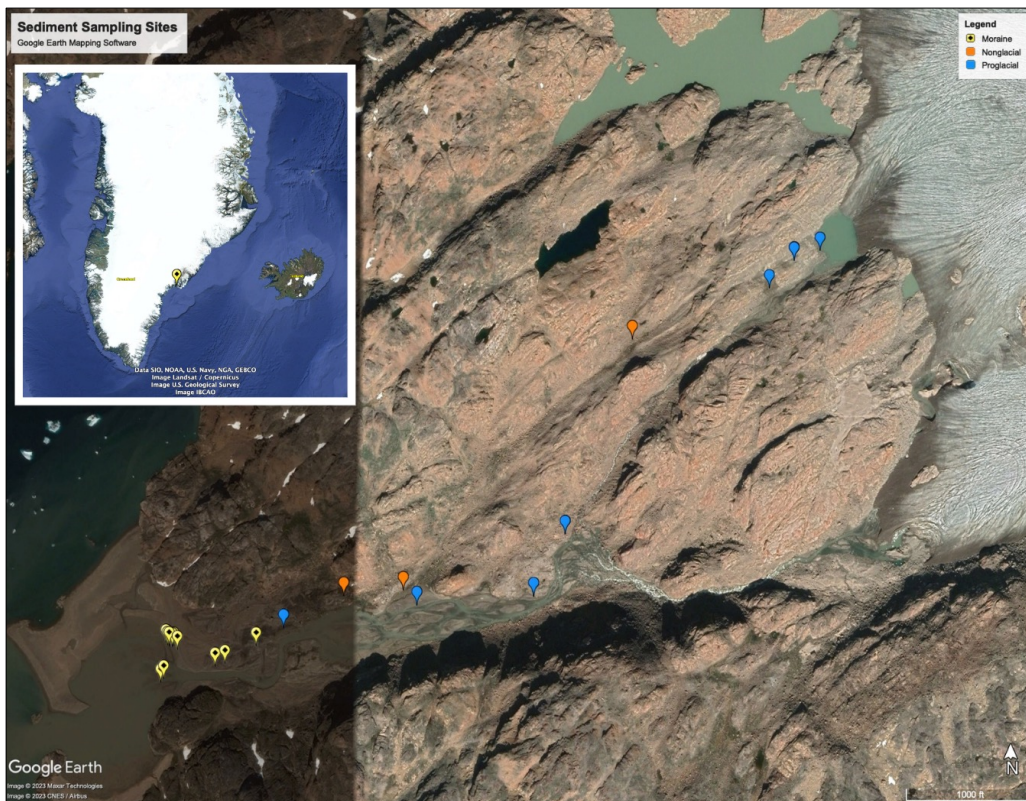


Figure 1. Map of sampling sites in relation to the glacier front.

Site Name	Distance from Glacier (miles)
<b>Nonglacial Sites</b>	
Serm NG 3 bedload	0.410
Serm NG1	0.800
Serm NG2	0.890
<b>Moraine Sites</b>	
Serm 2 till	0.550
SERM-MOR-F-E	1.031
SERM-MOR-A	1.080
SERM-MOR-C	1.100
SERM-MOR-C-surface	1.100
SERM-MOR-E-E	1.140
Serm-MOR-E-W	1.150
Serm-MOR-E-surface	1.150
Serm-MOR-F-surface	1.151
SERM-MOR-G-E	1.151
Serm-MOR-G-surface	1.151
Serm-MOR-G-W	1.151
Serm-MOR-D-NE	1.160
SERM-MOR-D-SW	1.180
<b>Proglacial Sites</b>	
Sermilik D bedload	0.110
Sermilik 1 bedload	0.150
Serm1	0.150
Serm 0	0.150
Serm 4 bedload	0.200
Sermilik 2	0.550
Sermilik A	0.610
Sermilik B	0.780
Sermilik C	0.980

Table 1. Glacial proximity to each sampling site.

### *Sample Collection*

Sediment samples were collected from nonglacial streams, proglacial streams, and moraines adjacent to the Mittivakkat Gletscher in southeast Greenland by Dr. Kelly Deuerling & colleagues from the locations shown in Figure 1. Samples were collected in Whirl-Pak® bags using gloved hands or a plastic trowel and stored at 4°C until processing.

### *Sample Processing*

Sediment samples were dried in a 105° C oven to remove moisture for 48 hours and allowed to cool. Then, each sample was split using a Rifle Particle Splitter to obtain homogeneous samples from the archive. These split samples were put through a 2 mm sieve to eliminate large rocks. Two portions of 8 grams each of the sieved samples were obtained from each distinct location, so that each site could be analyzed in duplicate. The 8 grams of sample were then added to a 50 mL Falcon tube along with 40 mL of deionized water, for a ratio of 1:5 parts sediment to fluid. Two tubes containing only deionized water (48 mL) were also included in the analysis as procedural blanks. Once the water was added to the tubes, they were placed onto a rotating wheel at 50 RPM to maintain homogenous movement.

Samples were leached for 24 hours. Then, the sample tubes were moved to a centrifuge where they were spun down at 2000 RPM to separate the solid and liquid portions. The resulting supernatant was removed using a syringe and pushed through a 0.45 µm filter to remove any suspended clay particles. This filtered supernatant was then divided into two equal portions and transferred into scintillation vials, one for anion analysis and one for cation analysis. The vials were then returned to 4°C storage.

### *Ion Chromatography Analysis*

The samples were analyzed on a Metrohm ion chromatograph with a Metrosep C 4 100/4.0 column for major cations ( $\text{Na}^+$ ,  $\text{K}^+$ ,  $\text{Mg}^{2+}$ ,  $\text{Ca}^{2+}$ ,  $\text{Li}^+$ ,  $\text{NH}_3^+$ ) and a Metrosep A Supp 4 250/4.0 column for major anions ( $\text{Cl}^-$ ,  $\text{F}^-$ ,  $\text{Br}^-$ ,  $\text{SO}_4^{2-}$ ,  $\text{NO}_2^-$ ,  $\text{NO}_3^-$ ,  $\text{PO}_4^{3-}$ ). Calibration curves for both the anion and cation analysis were determined using custom multi-element standards and verified between runs with a check standard. The eluents used for the anion analysis included a solution of 0.1 M sulfuric acid and a solution of 2.4 mM sodium bicarbonate and 2.5 mM sodium carbonate. The eluent used for the cation analysis included 2.2 mM nitric acid and 0.9 mM dipicolinic acid. All eluents were generated using 18 M $\Omega$  water to eliminate extraneous elemental presence. All check standards were with 10% of expected values.

#### *Data Processing*

All ion values were converted into milliequivalents per gram (meq/g). This represents the milliequivalent of analyte eluted per gram of solid sample leached. These units allow for a direct comparison of the values across all ions. The relative percent difference for each analyte in each pair of procedural duplicates was calculated. Four of the samples had a relative percent difference greater than 50%: Serm-Ng-1, Serm-Mor-A, Serm-Mor-G-Surface, and Sermilik B. These samples will require reanalysis at a later date. The duplicates were averaged to obtain an average meq/g value for each ion. These values are tabulated in Appendix 1.

### Results

Figure 2 includes standard cation and anion ternary plots. The anion ternary plot contains measured values for  $\text{Cl}^-$  and  $\text{SO}_4^{2-}$ , but calculated values for  $\text{HCO}_3^-$ . Acknowledging the limitations on the bicarbonate variable means this ternary plot may not fully reflect the sample



sites; however, the general patterns are likely consistent with environmental reality. The cation ternary plot contains measured values for all ions. The cation plot shows distinct clustering of the proglacial sites (blue) and the moraine sites (yellow). The anion plot shows similar clustering. The nonglacial sites do not show a distinct pattern, but all of their values fall within the range encompassed by both the proglacial and moraine sites for both ternaries.

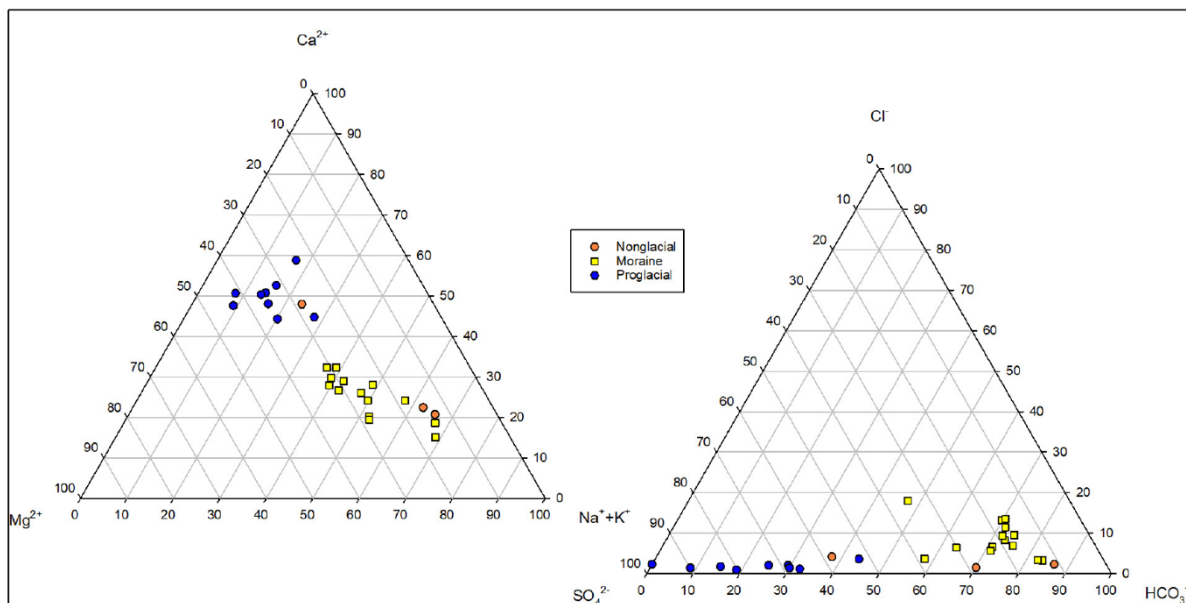


Figure 2. Ternary plots comparing major cations (left) and anions (right) from sediment leachate.

Figure 3 shows that sample sites closer to the glacier had more total dissolved solids (TDS) than sites further from the glacier. A statistical t-test analysis between proglacial TDS and moraine TDS yielded a p-value of 0.0001 ( $\alpha=0.05$ ). This indicates that the elevated TDS in the proglacial samples compared to the moraines was statistically significant.

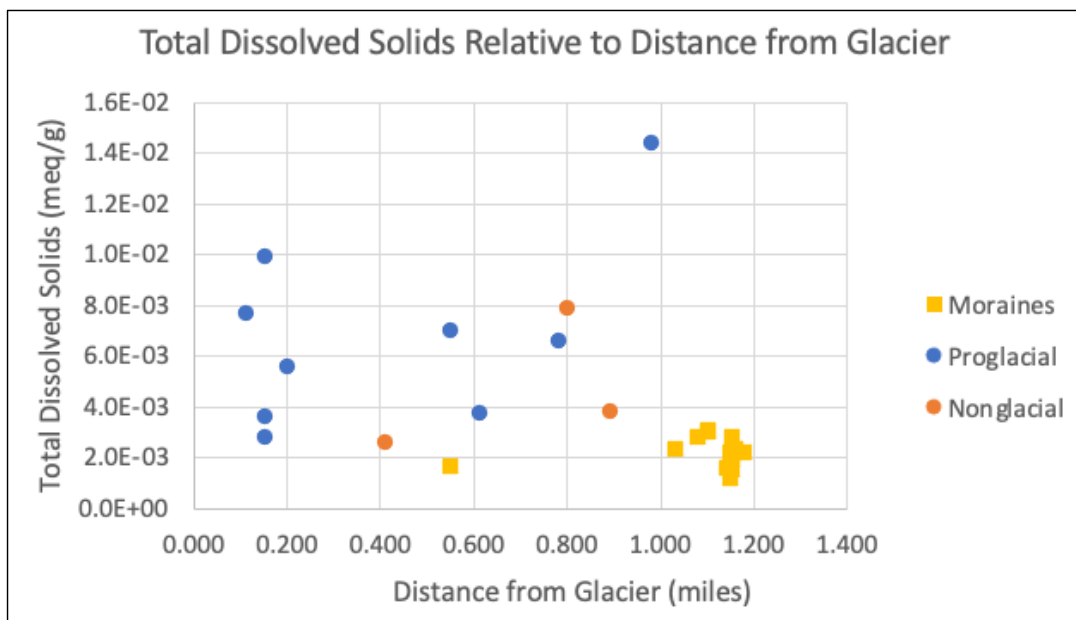


Figure 3. The amount of total dissolved solids in the leachate based on distance from the glacier, sorted by sediment type.

Figure 4 shows the ratio of Na:Cl for all sites. Seawater has a Na:Cl ratio of 0.86, as indicated by the solid line. Halite (NaCl) has a ratio of 1.00, as indicated by the dashed line. Data points above the solid line (trending towards the halite line) are indicative of an additional source of sodium beyond what is derived from sea spray. All of the proglacial sites and all but two of the moraine sites roughly parallel the seawater trend, whereas the nonglacial sites show divergence from this pattern.

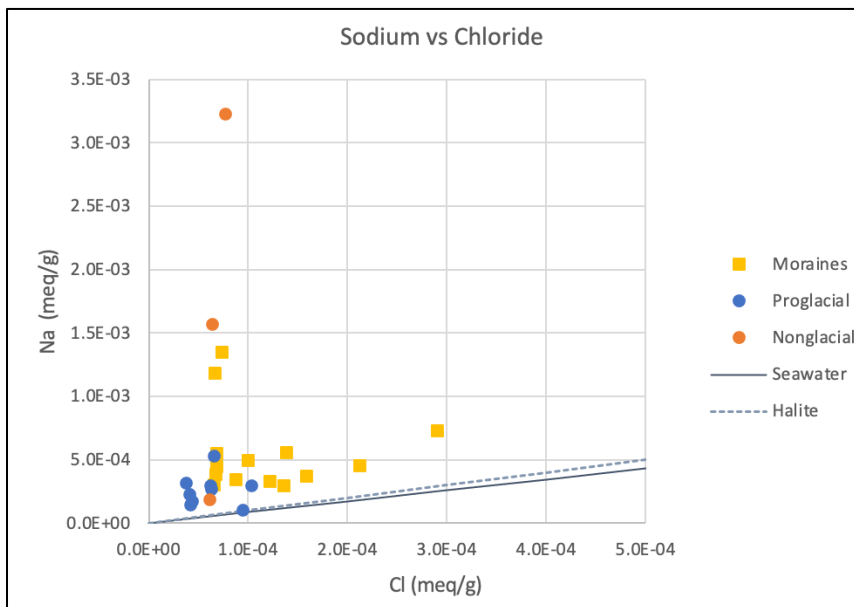


Figure 4. Comparison of Na and Cl abundance across all sites, compared with the Na:Cl ratio of seawater and halite.

Figure 5 shows the concentrations of calcium and sulfate in each sample. The 1:1 ratio line indicates the expected ratio for the weathering of gypsum ( $\text{CaSO}_4 \cdot 2\text{H}_2\text{O}$ ). The moraine sediments fall along the line, but proglacial sites are enriched in sulfate.

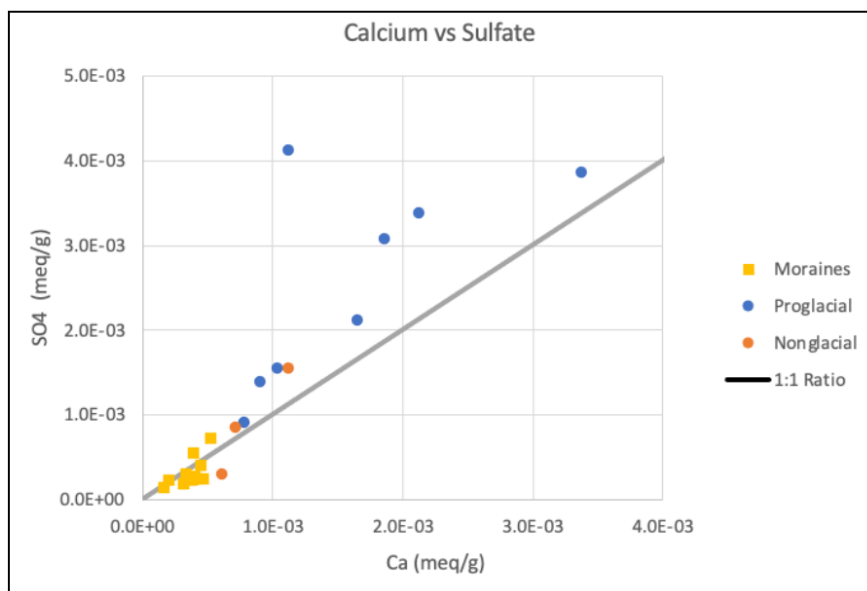


Figure 5. Comparison of calcium and sulfate ion concentrations from sediment leachate.

Figure 6 shows the ratios of calcium and magnesium in each sample. The 1:1 ratio line indicates the expected ratio for the weathering of dolomite ( $\text{CaMg}(\text{CO}_3)_2$ ). The moraines align with these ratios. The proglacial sites are enriched in calcium.

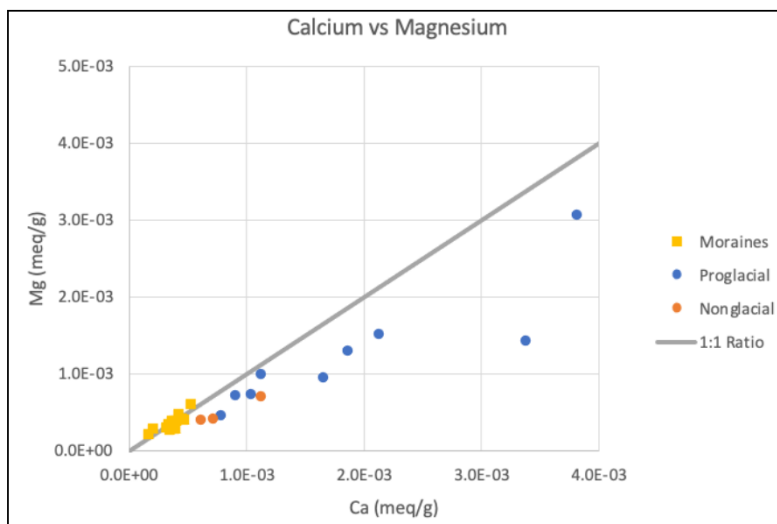


Figure 6. Comparison of calcium and magnesium ion concentrations from sediment leachate.

## Discussion

### Elemental Patterns

The general separation of proglacial and moraine sites on both plots in Figure 2 is indicative of divergent patterns in chemical weathering based on glacial proximity and glacial hydrologic interaction. For the cation plot specifically, the calcium dominance demonstrated in the proglacial sites is consistent with the knowledge that calcite will be preferentially weathered in a glacial system (Li et al., 2022). The enriched  $\text{Na}^+$  and  $\text{K}^+$  relative to  $\text{Mg}^{2+}$  and  $\text{Ca}^{2+}$  in moraine samples can be explained by their proximity to the coast and the influence of sea salt aerosol. For the anion ternary plot, the proglacial sites are enriched in sulfate, which is

related to the anoxic glacial environment. The distinct grouping of the moraine sites and the proglacial sites on both plots again confirms the theory of divergence in weathering.

As seen in Figure 3, proglacial sites likely show increased TDS because these sites are directly affiliated with glacial stream weathering. Moraine sites have been exposed to weathering processes for longer periods of time, and therefore have fewer available ions to leach out than the proglacial sites. The moraines are also no longer directly associated with glacial hydrology. Therefore, the pattern of salt weathering and deposition looks different in these sites than it would in a proglacial site, where salts are generated from evaporating glacial water.

As for the Na:Cl ratios observed in the samples, closer proximity to the seawater line in Figure 4 is indicative that sea spray deposits are likely the major contributor of  $\text{Na}^+$  and  $\text{Cl}^-$  ions in these sediments. Sites where these ions are further from the line have a different Na:Cl ratio than would be expected in seawater. All of the data points lie above the seawater line: they contain elevated sodium compared to what is found in seawater. Thus, it can be assumed this sodium is not from oceanic sources, but rather from the weathering of sodium-rich salts. (Neal & Kirchner, 2000).

Plagioclase, a feldspar, is a major mineral identified in the rocks of the Ammassalik Intrusive Complex. Plagioclase is a primary mineral formed from the crystallization of magma, with a composition ranging between  $\text{CaAl}_2\text{Si}_2\text{O}_8$  and  $\text{NaAlSi}_3\text{O}_8$ . The variance in composition is related to differences in crystallization temperatures (Nesse, 2018). Plagioclase is a likely source of sodium *in situ* in this region. Plagioclase minerals, especially in their more sodium-rich forms, are not quickly weathered in Earth surface environments (Goldich, 1938). Therefore, there is no

weathering of plagioclase expected to have occurred during this 24-hour leaching experiment. However, the incongruent weathering of feldspars and other minerals releases cations (including  $\text{Na}^+$ ) into the environment. This effect is amplified in glacial environments (Hodson, Tranter & Vante, 2000). These sodium ions, released through chemical weathering and sequestered as secondary precipitates in the bulk sediment samples, are likely the source of the excess  $\text{Na}^+$  generated in these samples. Therefore, although this sodium was originally derived from the plagioclase, the ions that were leached are those that were weathered and deposited again as salts in the sediment prior to collection for this study. These salts occur in multiple forms in addition to halite. A likely form for these secondary precipitates is  $\text{Na}_2\text{SO}_4$ , especially because of the enriched sulfates found in this region as well.

The elevated sulfate concentrations of proglacial leachate is likely a result of the anoxic subglacial environment. The longer flow paths under a glacier generate lower oxygen environments. This allows for the dissolution of sulfide minerals. The  $\text{S}^{2-}$  that is generated is pushed into the glacial foreland, where it gets oxidized into  $\text{SO}_4^{2-}$ . This enrichment in sulfate, strongly observed in the proglacial samples in this study, is represented in both Figure 2 and Figure 5.

The source of enriched calcium observed in the proglacial sites in Figure 5 is presumed to be from calcite weathering ( $\text{CaCO}_3$ ). Calcite is a softer mineral than dolomite, and so the physical erosion caused by glacial movement will increase the available sites for chemical weathering of calcite at a greater rate than dolomite. (Li et al., 2022). Additionally, calcite is one of the first phases to precipitate out during glacial cryoconcentration (Tranter, 2003). Therefore, the regions that these sediments were sampled from would have precipitated calcite

as the pore waters dried up, which would then be easily leached using this experimental process. Because the moraine sites fall along the line in Figure 4, it is expected that gypsum ( $\text{CaSO}_4 \cdot 2\text{H}_2\text{O}$ ) dissolution is the primary source of these two ions in these locations.

#### *Broader Weathering Trends*

The elemental composition of sediment weathering products differed markedly based on the site of origin. Differences were observed as a function of glacial proximity, as well as a function of hydrologic relationships to the glacier. These trends were observable within recently deglaciated regions, indicating the formation of an environmental gradient between the glacier front and the coast. Elevated ionic abundance in proglacial sites further from the coast aligns with the understanding that exposed moraine sites have been experiencing weathering conditions for a longer period. Although the total particle size distribution for the samples has not been analyzed, qualitative observations revealed finer particle sizes in proglacial sediments. This matches physical weathering patterns that are known to occur with glacial movement. As glaciers move across the landscape, the pressure exerted generates fine-grained, comminuted sediment. This sediment is relatively reactive. This chemical reactivity is related to the increased specific surface area due to the small particle size. It is also related to the emergence of the sediment from subglacial conditions into atmospheric weathering conditions. These processes accelerate chemical weathering fluxes (Anderson, 2005 & Deuerling et al., 2019).

#### *Implications*

Chemical weathering of carbonate and silicate minerals assists in controlling the concentration of atmospheric carbon dioxide. Prior to anthropogenic activities, interactions

between mineral weathering and geothermal activity maintained a balance of greenhouse gases. Atmospheric carbon dioxide reacts with water to form carbonic acid, which enables mineral weathering and acts as a pH buffer in ocean systems. The potential for chemical weathering is accelerated by physical erosion of glacial retreat. (Neal, 2009).

The differential weathering demonstrated in this study indicates potential variation in the drawdown of atmospheric carbon. The weathering of gypsum in the moraine samples is disconnected from the carbon cycle compared to the weathering of silicates. The places that are presently connected to water systems are likely undergoing incongruent silicate weathering, leading to elemental signatures different than those expected than if the solutes were derived directly from the dissolution of major mineral constituents (1:1 Ca:SO<sub>4</sub> for gypsum and 1:1 Ca:Mg for dolomite). The leachates measured in this study were derived from secondary minerals found in the pore spaces of the sediments. Glacial cryoconcentration leads to an increase in the solute concentrations in pore water, impacting the formation of these secondary minerals (Deuerling et al., 2018). Further analysis of the leachate and *in situ* water samples will provide greater insight into these patterns.

Weathering products also affect other biogeochemical cycles. For example, the increase of bioavailable ions along the glacier front have provided the nutrients required for new species of pigmented microalgae to grow. These microalgae have not been associated with rock weathering processes before. These species are elevating the local blackbody effect, which increases heat absorption— this in turn accelerates glacial melt further (Chevrollier et al., 2023, Halbach et al., 2022).



As glacial retreat accelerates, understanding the chemical reactions that are taking place as a result will assist researchers in modeling potential outcomes. In conjunction with the current body of knowledge regarding chemical weathering and its relationships to environmental patterns, scientists can make more accurate predictions about how changing climactic conditions will impact the Earth.

### Conclusion

The trends observed in the elemental composition of the leachates were consistent with the expected environmental gradients generated by glacial retreat. The formation of the chronosequence is evidence that glacial meltwater has discernable impacts on sediment weathering processes. It also demonstrates that these impacts are observable within areas that were deglaciated within the past 200 years. Leachate from moraine locations showed evidence of secondary gypsum and dolomite dissolution, as well as sodium and chloride input from sea spray. Proglacial sites showed divergence from these trends, demonstrating differential weathering related to glacial hydrology. The proglacial sites also contained evidence for increased calcite weathering. The observed patterns are useful in understanding glacial biogeochemical cycles. There is potential to apply this weathering information to models of deglaciation to assist in predicting future environmental conditions along the glacier front.

## References

- Anderson, Suzanne Prestrud (2005) Glaciers show direct linkage between erosion rate and chemical weathering fluxes, *Geomorphology*, Volume 67, Issues 1–2, Pages 147-157, ISSN 0169-555X, <https://doi.org/10.1016/j.geomorph.2004.07.010>.
- Beal, S. A. (2009). Chemical weathering along the Greenland Ice Sheet margin (Doctoral dissertation, Wheaton College; Norton, Mass.).
- Bhatia, M., Kujawinski, E., Das, S. et al. (2013) Greenland meltwater as a significant and potentially bioavailable source of iron to the ocean. *Nature Geosci* **6**, 274–278. <https://doi.org/10.1038/ngeo1746>
- Chevrollier, L. A., Cook, J. M., Halbach, L., Jakobsen, H., Benning, L. G., Anesio, A. M., & Tranter, M. (2023). Light absorption and albedo reduction by pigmented microalgae on snow and ice. *Journal of Glaciology*, 69(274), 333-341. <https://doi.org/10.1017/jog.2022.64>
- Deuerling, K. M., Martin, J.B., Martin, Ellen E., Scribner, C.A. (2018) Hydrologic exchange and chemical weathering in a proglacial watershed near Kangerlussuaq, west Greenland, *Journal of Hydrology*, Volume 556, Pages 220-232, ISSN 0022-1694, <https://doi.org/10.1016/j.jhydrol.2017.11.002>.
- Deuerling, K. M., Martin, J.B., Martin, Ellen E., Abermann, J., Myreng, S.M., Petersen, D., Rennermalm, Å.K. (2019) Chemical weathering across the western foreland of the Greenland Ice Sheet, *Geochimica et Cosmochimica Acta*, Volume 245, Pages 426-440, ISSN 0016-7037, <https://doi.org/10.1016/j.gca.2018.11.025>.

- Ernstsen, V. B. (2023). The Sermilik Scientific Research Station. Department of Geosciences and Natural Resource Management. Retrieved April 8, 2023, from <https://ign.ku.dk/english/about/field-stations/sermilik-station/>
- Goldich, S. S. (1938). A Study in Rock-Weathering. *The Journal of Geology*, 46(1), 17–58. <http://www.jstor.org/stable/30079586>
- Halbach, L., Chevrollier, L. A., Doting, E. L., Cook, J. M., Jensen, M. B., Benning, L. G., Bradley, J. A., Hansen, M., Lund-Hansen, L. C., Markager, S., Sorrell, B. K., Tranter, M., Trivedi, C. B., Winkel, M., & Anesio, A. M. (2022). Pigment signatures of algal communities and their implications for glacier surface darkening. *Scientific Reports*, 12, [17643]. <https://doi.org/10.1038/s41598-022-22271-4>
- Hawkings, J., Wadham, J., Tranter, M. et al. (2014) Ice sheets as a significant source of highly reactive nanoparticulate iron to the oceans. *Nat Commun* 5, 3929. <https://doi.org/10.1038/ncomms4929>
- Hawkings, J.R., Wadham, J.L., Tranter, M., Lawson, E., Sole, A., Cowton, T., Tedstone, A.J., Bartholomew, I., Nienow, P., Chandler, D., Telling, J. (2015) The effect of warming climate on nutrient and solute export from the Greenland Ice Sheet. *Geochem. Persp. Let.* 1, 94-104.
- Hodson, A., Tranter, M. and Vatne, G. (2000), Contemporary rates of chemical denudation and atmospheric CO<sub>2</sub> sequestration in glacier basins: an Arctic perspective. *Earth Surf. Process. Landforms*, 25: 1447-1471. [https://doi.org/10.1002/1096-9837\(200012\)25:13<1447::AID-ESP156>3.0.CO;2-9](https://doi.org/10.1002/1096-9837(200012)25:13<1447::AID-ESP156>3.0.CO;2-9)

- Li, X., Wang, N., Ding, Y. *et al.* (2022) Globally elevated chemical weathering rates beneath glaciers. *Nature Communications* 13, 407 (2022). <https://doi.org/10.1038/s41467-022-28032-1>
- Neal, C. and Kirchner, J. W. (2000). Sodium and chloride levels in rainfall, mist, streamwater and groundwater at the Plynlimon catchments, mid-Wales: inferences on hydrological and chemical controls, *Hydrol. Earth Syst. Sci.*, 4, 295–310, <https://doi.org/10.5194/hess-4-295-2000>
- Nesse, W. D. (2018). *Introduction to Mineralogy* (3rd ed.). Oxford University Press.
- Pedersen, M., Weng, W. L., Keulen, N., & Kokfelt, T. F. (2013). A new seamless digital 1:500 000 scale geological map of Greenland. *GEUS Bulletin*, 28, 65–68.  
<https://doi.org/10.34194/geusb.v28.4727>
- Tranter, M. (2003) 5.07 - Geochemical Weathering in Glacial and Proglacial Environments, Editor(s): Heinrich D. Holland, Karl K. Turekian, *Treatise on Geochemistry*, Pergamon, Pages 189-205, ISBN 9780080437514, <https://doi.org/10.1016/B0-08-043751-6/05078-7>.
- Varliero, G., Anesio, A. M., & Barker, G. L. (2021). A taxon-wise insight into rock weathering and nitrogen fixation functional profiles of proglacial systems. *Frontiers in Microbiology*, 12. <https://doi.org/10.3389/fmicb.2021.627437>
- Wadham, J., Tranter, M., Skidmore, M., Hodson, A., Priscu, J., Lyons, W., Sharp, M., Wynn, P. & Jackson, M. (2010). Biogeochemical weathering under ice: Size matters. *Global Biogeochem. Cycles*. 24. [10.1029/2009GB003688](https://doi.org/10.1029/2009GB003688).

Yu, S., Lv, J., Jiang, L., Geng, P., Cao, D., & Wang, Y. (2023). Changes of soil dissolved organic matter and its relationship with microbial community along the Hailuoguo Glacier Forefield Chronosequence. *Environmental Science & Technology*, 57(9), 4027–4038.  
<https://doi.org/10.1021/acs.est.2c08855>

Appendix 1

meq/g sediment ->	Fluoride	Chloride	Nitrite	Bromide	Nitrate	Phosphate	Sulfate	Lithium	Sodium	Ammonium	Potassium	Calcium	Magnesium	TDS	Distance from Glacial Front (miles)
Serm NG 3 bedload	4.1E-05	6.1E-05	1.8E-06	6.9E-07	7.4E-05	0.0E+00	8.6E-04	0.0E+00	1.9E-04	9.6E-05	1.6E-04	7.1E-04	4.2E-04	2.6E-03	0.410
Serm NG1*	0.0E+00	7.7E-05	2.6E-06	6.5E-07	6.7E-05	0.0E+00	1.5E-03	4.5E-05	3.2E-03	8.4E-04	2.9E-04	1.1E-03	7.1E-04	7.9E-03	0.800
Serm NG2	0.0E+00	6.3E-05	1.2E-05	2.2E-06	2.9E-04	2.2E-06	3.1E-04	2.2E-05	1.6E-03	3.7E-04	1.7E-04	6.1E-04	4.1E-04	3.8E-03	0.890
meq/g sediment ->	Fluoride	Chloride	Nitrite	Bromide	Nitrate	Phosphate	Sulfate	Lithium	Sodium	Ammonium	Potassium	Calcium	Magnesium	TDS	Distance from Glacial Front (miles)
Serm2 till	5.6E-05	6.8E-05	1.8E-05	2.0E-06	8.2E-06	0.0E+00	2.8E-04	0.0E+00	4.5E-04	5.3E-05	1.4E-04	3.4E-04	2.8E-04	1.7E-03	0.550
SERM-MOR-F-E	1.3E-04	2.1E-04	8.2E-06	2.2E-06	8.9E-06	0.0E+00	2.5E-04	2.5E-06	4.5E-04	1.7E-04	1.9E-04	4.1E-04	4.8E-04	2.3E-03	1.031
SERM-MOR-A*	3.7E-05	6.6E-05	4.1E-06	0.0E+00	4.9E-05	0.0E+00	2.7E-04	1.4E-05	1.2E-03	3.0E-04	1.7E-04	3.9E-04	3.0E-04	2.8E-03	1.080
SERM-MOR-C	4.2E-05	7.3E-05	0.0E+00	2.7E-07	4.6E-05	0.0E+00	3.1E-04	8.7E-06	1.4E-03	3.7E-04	1.7E-04	3.3E-04	3.5E-04	3.0E-03	1.100
SERM-MOR-C-surface	6.5E-05	6.8E-05	5.3E-06	6.0E-07	9.9E-05	0.0E+00	7.3E-04	2.5E-06	5.6E-04	2.3E-04	1.9E-04	5.2E-04	6.1E-04	3.1E-03	1.100
SERM-MOR-E-E	4.9E-05	1.4E-04	0.0E+00	8.0E-07	8.1E-05	0.0E+00	1.8E-04	0.0E+00	3.0E-04	1.0E-04	1.5E-04	3.1E-04	3.1E-04	1.6E-03	1.140
Serm-MOR-E-W	1.1E-04	8.7E-05	1.1E-06	1.9E-06	4.4E-05	0.0E+00	4.1E-04	0.0E+00	3.5E-04	2.2E-04	1.5E-04	4.4E-04	4.2E-04	2.2E-03	1.150
Serm-MOR-E-surface	6.2E-05	6.5E-05	0.0E+00	1.2E-06	3.2E-05	0.0E+00	1.5E-04	0.0E+00	3.0E-04	1.0E-04	1.0E-04	1.6E-04	2.2E-04	1.2E-03	1.150
Serm-MOR-F-surface	7.9E-05	6.7E-05	1.4E-06	1.6E-06	8.2E-06	0.0E+00	2.3E-04	0.0E+00	3.9E-04	1.4E-04	1.5E-04	2.0E-04	2.9E-04	1.6E-03	1.151
SERM-MOR-G-E	9.4E-05	1.6E-04	4.9E-06	1.3E-06	5.1E-05	6.4E-06	2.4E-04	4.0E-06	3.7E-04	1.3E-04	1.8E-04	4.6E-04	4.1E-04	2.1E-03	1.151
Serm-MOR-G-surface*	1.7E-04	2.9E-04	3.1E-06	1.1E-06	6.1E-05	1.2E-05	5.6E-04	5.7E-06	7.3E-04	1.3E-04	2.0E-04	3.9E-04	2.9E-04	2.8E-03	1.151
Serm-MOR-G-W	8.5E-05	1.2E-04	0.0E+00	1.5E-06	9.2E-05	0.0E+00	2.4E-04	0.0E+00	3.3E-04	1.2E-04	1.7E-04	3.8E-04	4.0E-04	1.9E-03	1.151
Serm-MOR-D-NE	1.1E-04	1.0E-04	2.1E-06	1.5E-06	8.5E-05	0.0E+00	2.6E-04	4.3E-06	5.0E-04	2.4E-04	2.1E-04	3.9E-04	4.0E-04	2.3E-03	1.160
SERM-MOR-D-SW	7.7E-05	1.4E-04	0.0E+00	1.3E-06	3.5E-05	0.0E+00	2.4E-04	1.0E-05	5.6E-04	2.0E-04	1.8E-04	3.6E-04	3.9E-04	2.2E-03	1.180
meq/g sediment ->	Fluoride	Chloride	Nitrite	Bromide	Nitrate	Phosphate	Sulfate	Lithium	Sodium	Ammonium	Potassium	Calcium	Magnesium	TDS	Distance from Glacial Front (miles)
Sermilik D bedload	0.0E+00	3.7E-05	5.7E-06	0.0E+00	4.6E-06	0.0E+00	3.4E-03	1.1E-05	3.2E-04	2.5E-05	2.5E-04	2.1E-03	1.5E-03	7.7E-03	0.110
Sermilik 1 bedload	1.3E-05	4.1E-05	0.0E+00	0.0E+00	3.4E-06	0.0E+00	1.4E-03	4.3E-06	2.3E-04	1.0E-04	1.9E-04	9.0E-04	7.2E-04	3.6E-03	0.150
Serm1	7.2E-05	6.6E-05	1.5E-06	0.0E+00	4.0E-05	0.0E+00	3.9E-03	5.0E-06	5.4E-04	1.2E-04	4.5E-04	3.4E-03	1.4E-03	1.0E-02	0.150
Serm 0	2.1E-05	6.2E-05	3.0E-06	0.0E+00	3.2E-05	0.0E+00	9.1E-04	0.0E+00	3.0E-04	7.7E-05	1.9E-04	7.7E-04	4.7E-04	2.8E-03	0.150
Serm 4 bedload	0.0E+00	4.3E-05	1.2E-06	0.0E+00	2.0E-04	0.0E+00	2.1E-03	2.5E-06	1.8E-04	1.7E-04	3.1E-04	1.6E-03	9.6E-04	5.6E-03	0.200
Sermilik 2	1.6E-05	6.3E-05	0.0E+00	0.0E+00	6.4E-05	0.0E+00	3.1E-03	0.0E+00	2.7E-04	1.3E-04	2.7E-04	1.9E-03	1.3E-03	7.1E-03	0.550
Sermilik A	9.3E-06	4.1E-05	0.0E+00	0.0E+00	2.3E-06	0.0E+00	1.5E-03	1.4E-06	1.5E-04	5.1E-05	1.9E-04	1.0E-03	7.4E-04	3.8E-03	0.610
Sermilik B*	6.3E-06	9.5E-05	0.0E+00	0.0E+00	5.2E-06	0.0E+00	4.1E-03	0.0E+00	1.1E-04	4.9E-05	1.0E-04	1.1E-03	1.0E-03	6.6E-03	0.780
Sermilik C	2.2E-05	1.0E-04	0.0E+00	0.0E+00	6.2E-06	0.0E+00	6.7E-03	5.4E-06	3.0E-04	8.8E-05	3.0E-04	3.8E-03	3.1E-03	1.4E-02	0.980

\*Indicates relative percent difference between duplicates over 50%

Table 2. The concentration of major cations and anions (meq/g) in sediment leachate for each site. Orange indicates nonglacial sites, yellow indicates moraine sites, and blue indicates proglacial sites. For more information regarding the geographic location of these sites, see Figure 1.